Sub-threshold Binary Neutron Star Search in Advanced LIGO's First Observing Run

Ryan Magee[1,2] , Heather Fong[3,4,5], Sarah Caudill[6], Cody Messick[1,2] , Kipp Cannon[3,5], Patrick Godwin[1,2], Chad Hanna[1,2,7,8], Shasvath Kapadia[9], Duncan Meacher[9], Siddharth R. Mohite[9,12], Debnandini Mukherjee[9], Alexander Pace[1,2], Surabhi Sachdev[1,2], Minori Shikauchi[10], and Leo Singer[11]

[1] Department of Physics, The Pennsylvania State University, University Park, PA 16802, USA
[2] Institute for Gravitation and the Cosmos, The Pennsylvania State University, University Park, PA 16802, USA
[3] Canadian Institute for Theoretical Astrophysics, 60 St. George Street, University of Toronto, Toronto, ON M5S 3H8, Canada
[4] Department of Physics, 60 St. George Street, University of Toronto, Toronto, ON M5S 3H8, Canada
[5] RESCEU, The University of Tokyo, Tokyo, 113-0033, Japan
[6] Nikhef, Science Park, 1098 XG Amsterdam, The Netherlands
[7] Department of Astronomy and Astrophysics, The Pennsylvania State University, University Park, PA 16802, USA
[8] Institute for CyberScience, The Pennsylvania State University, University Park, PA 16802, USA
[9] Leonard E. Parker Center for Gravitation, Cosmology, and Astrophysics, University of Wisconsin-Milwaukee, Milwaukee, WI 53201, USA
[10] Department of Astronomy, School of Science, The University of Tokyo, Hongo, Tokyo 113-0033, Japan
[11] NASA/Goddard Space Flight Center, Greenbelt, MD 20771, USA

Abstract

We present a search for gravitational waves from double neutron star binaries inspirals in Advanced Laser Interferometer Gravitational-Wave Observatory's (LIGO's) first observing run. The search considers a narrow range of binary chirp masses motivated by the population of known double neutron-star binaries in the nearby universe. This search differs from previously published results by providing the most sensitive published survey of neutron stars in Advanced LIGO's first observing run within this narrow mass range, and also including times when only one of the two LIGO detectors was in operation in the analysis. The search was sensitive to binary neutron star (BNS) inspirals to an average distance of ∼85 Mpc over 93.2 days. We do not identify any unambiguous gravitational wave signals in our sample of 103 sub-threshold candidates with false-alarm rates of less than one per day. However, given the expected BNS merger rate of $\mathcal{R} \approx 100\text{–}4000 \, \mathrm{Gpc}^{-3} \, \mathrm{yr}^{-1}$, we expect $\mathcal{O}(1)$ gravitational-wave events within our candidate list. This suggests the possibility that one or more of these candidates is in fact a BNS merger. Although the contamination fraction in our candidate list is ∼99%, it might be possible to correlate these events with other messengers to identify a potential multi-messenger signal. We provide an online candidate list with the times and sky locations for all events in order to enable multi-messenger searches.

Key words: catalogs – gravitational waves – stars: neutron

1. Introduction

Advanced Laser Interferometer Gravitational-Wave Observatory (LIGO; Aasi et al. 2015) conducted its first observing run (O1) from 2015 September 12 to 2016 January 19. Previous analyses of the 51.5 days of coincident LIGO Hanford and LIGO Livingston data led to three detections of binary black-hole mergers (Abbott et al. 2016a, 2016b, 2016c, 2018b; Nitz et al. 2019b). No binary neutron star (BNS) or neutron-star black-hole (NSBH) systems were observed (Abbott et al. 2016d) in O1. We revisit this data with a gravitational wave (GW) search targeted at BNS masses and provide a list of candidate events. Searches that catalog low signal-to-noise ratio (S/N) events probe significantly deeper into the cosmos. At low S/N it can be difficult to claim an unambiguous detection, but the multi-messenger nature of BNS systems (Abbott et al. 2017a) can be leveraged to identify authentic GW events. Comparisons of catalogs provide a discovery space for a host of multi-messenger signals (Smith et al. 2013; Burns et al. 2019). Temporal and/or spatial coincidences between candidates in distinct astrophysical channels could strongly support a multi-messenger discovery. Another potential application of this candidate list is to investigate fast radio bursts (FRBs). Some FRB origin theories are based on BNS merger and thought to be associated with GWs as well

(Totani 2013; Wang et al. 2016; Dokuchaev & Eroshenko 2017). FRBs are detected with accuracies of milliseconds, potentially allowing very tight coincidence windows in correlation studies between this catalog and arrival times of FRBs. This Letter will take the lead in this future GW follow-up search.

Most LIGO analyses have required two detectors to identify candidate GW events (Babak et al. 2013). In Advanced LIGO's O1, this requirement excluded nearly half of the available data[13] from analysis (Abbott et al. 2016c). Previous compact binary coalescence (CBC) searches using prototype LIGO (Allen et al. 1999) and TAMA300 (Tagoshi et al. 2001) data analyzed single-detector time. In O1, the PyCBC pipeline (Usman et al. 2016; Dal Canton & Harry 2017; Nitz et al. 2019a) cataloged single-detector triggers primarily for detector characterization purposes, and the search for GWs associated with gamma-ray bursts (Abbott et al. 2017b) also analyzed times with one operating interferometer. In Advanced LIGO's second observing run (O2), GW170817 was first identified as a LIGO Hanford trigger by the GstLAL online pipeline with an estimated false-alarm rate of ∼1/9000 yr (Essick et al. 2017). PyCBC Live also produced single-detector online triggers in O2 (Nitz et al. 2018). We include single-interferometer data in our search, and we assign significances to O1 single-detector

---

[12] LSSTC Data Science Fellow.

[13] Data that passes Category 1 data quality (DQ) checks. These DQ cuts eliminate ∼6% of coincident time.

candidates for the first time, although we note that others have previously suggested methods to rank these candidates (Cannon et al. 2015; Callister et al. 2017; Messick et al. 2017).

1-OGC (Nitz et al. 2019b) recently provided a catalog of GW candidates in O1 data obtained via the Gravitational Wave Open Science Center (GWOSC;[14] Vallisneri et al. 2015). The search presented here differs in several major ways. First, we target BNS systems exclusively by applying a mass model to increase sensitivity to those systems (Cannon et al. 2013; Fong 2018). Second, we use a denser grid of template waveforms to minimize signal loss caused by the discrete nature of the template bank (Owen 1996). Third, we include an additional 44.5 days of single-detector time in our analysis to increase the analyzed time and improve the sensitivity of the search. Fourth, we include additional coincident data that was not analyzed in 1-OGC. Finally, we include all candidates with false-alarm rates less than one per day in our list and we provide BAYESTAR (Singer & Price 2016) sky localization estimates for each candidate to encourage multi-messenger follow-up surveys.

2. Search Description

We used the GstLAL-based inspiral pipeline to conduct a matched-filter analysis (Allen et al. 2012; Cannon et al. 2012; Messick et al. 2017; GstLAL 2018; Gstreamer 2018; LIGO Scientific Collaboration 2018; Sachdev et al. 2019) of data provided by GWOSC and spanning 2015 September 12 to 2016 January 19. GWOSC data is only available for times that pass Category 1 data quality (DQ) checks (Abbott et al. 2018a), leaving 48.6 days of coincident data and 44.5 days of single-detector data. We exclude times known to have hardware injections from our analysis and apply no additional DQ cuts. Additional information on the DQ and hardware injections is available via GWOSC.

2.1. Template Bank

Matched-filter-based analyses correlate the data with a discrete bank of template waveforms (Owen & Sathyapra-kash 1999; Harry et al. 2009; Ajith et al. 2014) that model the GW emission of compact binaries (Blanchet et al. 1995; Ajith et al. 2007; Buonanno et al. 2009). The template bank used for this search was designed to maximize sensitivity to BNS mergers with component masses and spins motivated by double neutron star binary observations (Thorsett & Chakrabarty 1999; Ozel et al. 2012; Abbott et al. 2017c). For astrophysical reasons, we consider component spins that are purely aligned or anti-aligned with the orbital angular momentum, and we limit the dimensionless spin magnitude to be $\leqslant 0.05$ (Abbott et al. 2016e).

We model the component masses of our target population with a Gaussian distribution where $\bar{m} = 1.33 M_{\odot}$, $\sigma = 0.05 M_{\odot}$ (Ozel et al. 2012). We consider four standard deviations in mass and transform coordinates from component mass to chirp mass, $\mathcal{M} = (m_1 m_2)^{3/5}/(m_1 + m_2)^{1/5}$, as the chirp mass is the primary parameter that affects the GW signal (Finn & Chernoff 1993). We broaden the resulting chirp mass distribution to allow for statistical errors in our measurements and we increase the mean of the distribution to account for
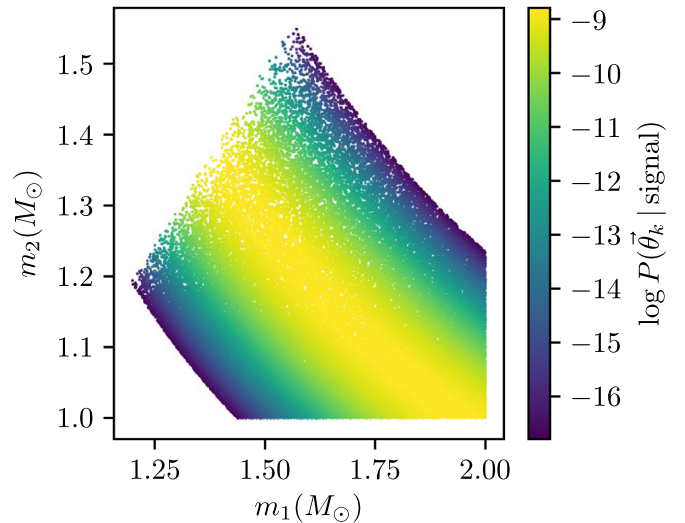
Figure 1. Template bank used for this search as depicted in component masses, m_1, m_2, where $m_1 > m_2$. The colors represent the logarithm of probability that a signal is recovered by a template t_k (with parameters $\boldsymbol{\theta}$); for this search, we have chosen a BNS population model with a mean mass of $\bar{m} = 1.33 M_{\odot}$ and a standard deviation of $\sigma = 0.05 M_{\odot}$. The population model considers three standard deviations in chirp mass. Although this population model neglects effects due to redshift, redshift effects are considered when we estimate the sensitivity of the search.

redshift. This results in a target population with detector frame chirp masses of $\mathcal{M} \in (1.04 M_{\odot}, 1.36 M_{\odot})$.

We first construct a template bank for $1 M_{\odot} < m_1$, $m_2 < 2 M_{\odot}$ with the TaylorF2 approximant. We impose a minimum match of .99, which ensures that signals with arbitrary parameters have a 99% match with at least one template in the bank. This high precision limits the loss of signals due to the use of a discrete template bank to $\sim 3\%$; previous searches in O1 data have used template banks that allowed signal loss up to $\lesssim 10\%$ (Dal Canton & Harry 2017; Mukherjee et al. 2018; Nitz et al. 2019b). After constructing the preliminary bank, we discard all templates that fall outside of the target chirp mass range. This results in a bank of 65,634 template waveforms.

2.2. Estimating Significance of Events

We use a likelihood-ratio statistic, $\mathcal{L}$, to rank candidate events by their S/N, an autocorrelation-based signal consis-tency check, the sensitivity of each detector at the time of the candidate, and the time and phase delays between different GW observatories (Cannon 2008; Cannon et al. 2013, 2015; Dent & Veitch 2014; Messick et al. 2017; Hanna et al. 2019; Sachdev et al. 2019). In addition, we include an astrophysical prior, which provides the probability that a signal from a BNS source population is recovered by a particular template (Fong 2018). The template bank and the prior probabilities associated with each template are shown in Figure 1.

Candidate events are assigned a false-alarm rate that describes how often a candidate with a likelihood-ratio statistic at least as high as its own is expected to occur; the false-alarm rate thus acts as a measure of how often the noise can be expected to produce a candidate with similar properties. The first GW detections had an extremely low false-alarm rate (less than $1/100{,}000$ yr). Here we are interested in digging considerably deeper into the noise-probing events with false-alarm rates as high as $1 \, \mathrm{day}^{-1}$.

Table 1
BNS Triggers from Advanced LIGO's O1 with a False-alarm Rate of Less than One Per Day

Date	False-alarm Rate (yr^{-1})	S/N	p-astro	Area (deg^2)
2015 Sep 14T18:35:13.66[H]	145.45	8.59	3.75×10^{-3}	24222
2015 Sep 18T06:38:39.21	261.92	8.04	2.18×10^{-3}	3150
2015 Sep 18T22:47:27.39†	193.46	8.52	2.92×10^{-3}	2624
2015 Sep 19T00:05:01.08†	326.71	7.63	1.78×10^{-3}	3161
2015 Sep 21T10:10:02.92[H]	7.52	8.10	6.95×10^{-2}	24235
2015 Sep 22T11:26:08.35	312.67	8.61	1.86×10^{-3}	3322
2015 Sep 23T13:47:35.79	165.39	8.56	3.38×10^{-3}	2008
2015 Sep 24T00:53:02.68	19.68	8.45	2.29×10^{-2}	2297
2015 Sep 24T05:57:35.24	107.32	8.71	4.88×10^{-3}	1367
2015 Sep 25T01:24:33.74	56.59	9.15	8.73×10^{-3}	2073
2015 Sep 25T21:15:15.92	38.39	8.58	1.25×10^{-2}	1906
2015 Sep 26T23:51:25.50	56.05	8.39	8.81×10^{-3}	2269
2015 Sep 27T14:28:55.77	243.80	8.60	2.32×10^{-3}	1826
2015 Sep 29T01:46:01.42†	251.32	8.50	2.26×10^{-3}	2248
2015 Sep 29T12:25:33.33	358.03	8.64	1.62×10^{-3}	1886
2015 Oct 01T00:21:02.89	293.57	8.70	1.97×10^{-3}	2385
2015 Oct 01T05:32:40.37	15.49	8.94	2.83×10^{-2}	2189
2015 Oct 02T01:49:03.99	118.27	9.21	4.49×10^{-3}	2032
2015 Oct 02T04:01:03.45	190.83	8.99	2.96×10^{-3}	1861
2015 Oct 04T22:32:11.75[H]	30.52	8.17	1.53×10^{-2}	24231
2015 Oct 05T07:12:04.91	104.11	8.46	5.02×10^{-3}	2958
2015 Oct 05T22:29:34.31	139.59	8.24	3.88×10^{-3}	2098
2015 Oct 09T23:08:05.70	292.60	8.19	1.98×10^{-3}	2471
2015 Oct 12T02:40:22.39	142.27	8.42	3.82×10^{-3}	2321
2015 Oct 12T14:26:43.18	322.93	8.35	1.80×10^{-3}	2656
2015 Oct 13T14:29:57.73[H]	37.36	9.02	1.28×10^{-2}	24221
2015 Oct 14T05:29:42.91†	149.36	8.75	3.68×10^{-3}	2756
2015 Oct 18T19:03:46.85[H]	7.52	8.05	0.181	24238
2015 Oct 19T17:37:05.25	124.01	8.78	4.30×10^{-3}	2046
2015 Oct 24T09:01:50.34[L]	94.09	10.56	5.53×10^{-3}	24218
2015 Oct 24T09:03:52.00[L]	7.52	9.69	7.96×10^{-2}	24218
2015 Oct 24T19:53:05.66	360.26	8.57	1.61×10^{-3}	1707
2015 Oct 28T12:24:31.67[H]	7.52	9.06	0.181	24221
2015 Oct 28T17:03:45.19†	16.08	8.82	2.74×10^{-2}	2100
2015 Oct 28T17:05:21.17†	0.78	10.63	0.289	1384
2015 Oct 29T08:27:29.92	345.02	9.04	1.68×10^{-3}	2209
2015 Oct 29T11:48:01.64	58.64	8.78	8.45×10^{-3}	2305
2015 Oct 29T12:05:48.00	363.99	8.24	1.59×10^{-3}	2146
2015 Oct 29T19:18:33.06	193.47	8.26	2.92×10^{-3}	2268
2015 Oct 30T00:08:56.47	358.38	8.55	1.62×10^{-3}	2593
2015 Oct 30T04:08:58.11	240.56	8.44	2.35×10^{-3}	2505
2015 Oct 31T10:27:43.77	320.37	8.05	1.81×10^{-3}	2891
2015 Oct 31T11:30:36.72	329.59	8.35	1.76×10^{-3}	2867
2015 Oct 31T22:01:00.91[L]	331.06	7.97	1.76×10^{-3}	24240
2015 Nov 01T11:13:23.94[L]	12.17	8.65	3.50×10^{-2}	24223
2015 Nov 04T13:37:23.67†	103.50	8.43	5.05×10^{-3}	1881
2015 Nov 04T15:16:09.12†	69.89	9.12	7.23×10^{-3}	1877
2015 Nov 05T06:20:44.61	312.42	8.56	1.86×10^{-3}	2577
2015 Nov 06T07:44:18.43	95.56	8.42	5.45×10^{-3}	2155
2015 Nov 06T10:07:13.79†	172.79	8.55	3.25×10^{-3}	2527
2015 Nov 06T11:05:19.24	211.28	9.18	2.67×10^{-3}	1231
2015 Nov 06T22:32:34.11	190.79	8.33	2.96×10^{-3}	820
2015 Nov 10T00:32:55.28†	313.96	8.86	1.85×10^{-3}	2309
2015 Nov 12T20:56:57.33	287.61	8.63	2.01×10^{-3}	2288
2015 Nov 15T20:03:17.46	26.66	8.35	1.73×10^{-2}	2251
2015 Nov 15T23:04:35.21	359.97	8.42	1.61×10^{-3}	2455
2015 Nov 16T10:59:11.86	189.42	8.24	2.98×10^{-3}	2430
2015 Nov 17T06:34:02.07[H]	7.52	8.84	0.181	24221
2015 Nov 20T21:07:08.38†	15.60	8.95	2.81×10^{-2}	2562
2015 Nov 21T22:26:44.55	104.06	8.65	5.02×10^{-3}	2308
2015 Nov 26T13:34:13.65	6.09	8.68	6.23×10^{-2}	1869
2015 Nov 28T08:29:19.80	229.16	8.16	2.46×10^{-3}	2657
2015 Nov 28T14:05:27.32	128.85	8.55	4.16×10^{-3}	2096
2015 Nov 29T03:39:34.71	250.42	9.27	2.27×10^{-3}	1245

Table 1
(Continued)

Date	False-alarm Rate (yr^{-1})	S/N	p-astro	Area (deg^2)
2015 Dec 02T10:45:49.81	201.50	9.24	2.80×10^{-3}	2022
2015 Dec 02T15:17:48.11	308.63	9.28	1.88×10^{-3}	1798
2015 Dec 02T17:38:00.95†	363.08	8.14	1.60×10^{-3}	2090
2015 Dec 03T20:18:18.94	110.58	8.37	4.76×10^{-3}	2280
2015 Dec 04T01:53:39.14	225.02	9.09	2.50×10^{-3}	2909
2015 Dec 04T21:14:59.74†	8.89	9.04	4.57×10^{-2}	1757
2015 Dec 05T10:16:47.45	284.26	8.59	2.03×10^{-3}	2471
2015 Dec 06T06:50:38.17^L	77.45	7.72	6.64×10^{-3}	24264
2015 Dec 08T09:27:47.71	344.81	8.27	1.68×10^{-3}	2349
2015 Dec 08T13:22:36.24	47.36	8.76	1.03×10^{-2}	1060
2015 Dec 09T07:25:24.68	141.65	7.85	3.84×10^{-3}	2606
2015 Dec 14T18:15:44.85	145.53	8.43	3.75×10^{-3}	2467
2015 Dec 14T19:32:20.42	145.58	8.72	3.75×10^{-3}	1556
2015 Dec 15T06:04:29.41	20.34	8.49	2.23×10^{-2}	2286
2015 Dec 15T10:53:01.22	154.61	8.78	3.58×10^{-3}	2289
2015 Dec 18T00:56:19.12	83.80	8.19	6.19×10^{-3}	2880
2015 Dec 18T09:59:11.16	147.23	8.71	3.72×10^{-3}	2141
2015 Dec 20T05:33:58.81	300.99	7.86	1.92×10^{-3}	3224
2015 Dec 22T10:08:48.42	234.05	9.22	2.41×10^{-3}	849
2015 Dec 23T00:07:10.93	18.95	8.99	2.36×10^{-2}	1847
2015 Dec 23T12:23:35.72	60.11	10.25	8.26×10^{-3}	1568
2015 Dec 23T13:50:49.48	178.46	8.00	3.16×10^{-3}	2461
2015 Dec 23T16:13:55.82	290.02	8.98	1.99×10^{-3}	1699
2015 Dec 24T23:05:56.58	47.49	10.08	1.03×10^{-2}	1501
2015 Dec 24T23:06:28.51	146.99	9.55	3.72×10^{-3}	1644
2015 Dec 24T23:06:57.04	70.65	9.42	7.16×10^{-3}	1476
2015 Dec 25T02:16:31.87	320.05	8.49	1.82×10^{-3}	2284
2015 Dec 28T21:04:05.90^H	160.93	8.57	3.46×10^{-3}	24224
2015 Dec 29T11:50:15.09^H	234.41	8.23	2.41×10^{-3}	24229
2015 Dec 31T11:20:54.32^H	180.00	8.82	3.13×10^{-3}	24219
2016 Jan 02T02:47:29.35	356.13	7.51	1.63×10^{-3}	3487
2016 Jan 02T02:54:39.60	239.65	8.11	2.36×10^{-3}	868
2016 Jan 03T02:29:54.78†	237.44	8.56	2.38×10^{-3}	1912
2016 Jan 03T17:23:13.26	208.47	8.91	2.70×10^{-3}	1979
2016 Jan 08T09:21:19.61	136.59	8.89	3.95×10^{-3}	2274
2016 Jan 08T10:09:33.90†	218.62	8.52	2.58×10^{-3}	1511
2016 Jan 12T05:19:01.34	107.14	8.34	4.89×10^{-3}	2271
2016 Jan 15T08:37:05.94	328.35	8.19	1.77×10^{-3}	2393
2016 Jan 19T05:40:13.04†	228.18	8.85	2.47×10^{-3}	2452

Note. Events marked by and H, L were found as single-detector triggers in LIGO-Hanford or LIGO-Livingston, respectively. The area column Shows the size of the 90% confidence region. Events marked by a † occurred within 0.01 s of a trigger in 1-OGC (Nitz et al. 2019b). We expect $\mathcal{O}(1)$ of these candidates to be GWs.

To estimate the false-alarm rate for candidate events, we use triggers that are not found in temporal coincidence between the interferometers when both LIGO detectors were operating to estimate the background of noise-like events (Cannon et al. 2013, 2015; Messick et al. 2017). Single-detector events also have their background estimated from the set of non-coincident triggers found when both LIGO detectors were operating, which amounts to 48.6 days of data. The single-detector backgrounds are constructed independently for each detector; only Hanford triggers from coincident time inform the Hanford single-detector background. We estimate our background from the 48.6 days of coincident data. When a single-detector candidate has a higher likelihood ratio than any candidate in the background, we bound its false-alarm rate to 1/48.6 days.

2.3. Estimating the Sensitivity of the Search

The search sensitivity was estimated via Monte Carlo methods. We first generated a set of BNS signals arising from systems with parameters that are consistent with local populations—we chose a Gaussian distribution for the source component masses with $m_{\mathrm{mean}} = 1.33\,M_\odot$, $\sigma_m = 0.05\,M_\odot$ and an isotropic distribution for spin. The injected population was modeled to a redshift of $z = 0.2$, and probed a spacetime volume of $0.77\,\mathrm{Gpc}^3\,\mathrm{yr}$. We rejected 17,738,506 simulated signals that had S/Ns below 3 to reduce the number of compute cycles. The remaining 112,073 fake signals were injected into the data and subsequently searched for by the detection pipeline. At a given false-alarm-rate threshold, we estimate the overall sensitivity of the search via

$$\langle VT \rangle = \langle VT_{\mathrm{injected}} \rangle \frac{N_{\mathrm{recovered}}}{N_{\mathrm{total\ sims}}} \qquad (1)$$

where $N_{\mathrm{recovered}}$ varies with the false-alarm-rate threshold. This search is approximately 30% more sensitive at the 1/100 yr threshold than the previous BNS search presented at the end of Advanced LIGO's O1 (Abbott et al. 2016d). The inclusion of single-detector time in our analysis leads to a ~33% improvement in our estimated $\langle VT \rangle$ at the 1 day^{-1} level.

3. Results

We find no unambiguous GW events, but we identify 103 candidates with false-alarm rates that are less than one per day. We provide the time, S/N, and false-alarm rate of each candidate in Table 1, as well as the probability that the candidate is astrophysical in origin (p_a). We compute p_a using FGMC methods (Cannon et al. 2015; Farr et al. 2015). When the p_a assigned to single-detector candidates via FGMC exceeds the estimated single-detector p_a bound in (Callister et al. 2017), we substitute the lower bound. The associated source parameters and sky localization estimates obtained via BAYESTAR (Singer & Price 2016) are provided on the LIGO Document Control Center at https://dcc.ligo.org/public/0158/P1900030/001/index.html.

Although we cannot identify any one candidate from our list as astrophysical, we can estimate the number of true signals buried in the list from our search sensitivity and the expected BNS merger rate. At a false-alarm-rate threshold of 1 day^{-1}, we estimate $\langle VT \rangle = 6.7 \times 10^5$ Mpc^3 yr. The LIGO Scientific Collaboration recently estimated the local merger rate of BNS systems to be $\mathcal{R} \approx 100$–4000 Gpc^{-3} yr^{-1} at 90% confidence (Abbott et al. 2018b); we adopt a nominal value of 1000 Gpc^{-3} yr^{-1}. We therefore expect that $\langle VT \rangle \times \mathcal{R} = 0.67^{+2.0}_{-.60}$ of the candidates presented here are GW signals from BNS coalescences. We stress that although the number of expected events depends on uncertainties in both $\langle VT \rangle$ and $\mathcal{R}$, the expected number remains at most $\mathcal{O}(1)$.

A single signal in our candidate list would imply a contamination fraction of 99%. We provide the coalescence times in Table 1 and approximate sky localizations online to encourage multi-messenger searches that have the ability to illuminate true signals buried in the candidate list.

4. Discussion

We have presented a search for GWs from BNS mergers. Although no GW signal was clearly identified in either single- or double-interferometer time, we have provided a list of candidate events with false-alarm rates that are less than one per day. The parameters for this search overlap with those of GW catalogs GWTC-1 (Abbott et al. 2018b) and 1-OGC (Nitz et al. 2019b). No shared events are found in O1 data between this candidate list and GWTC-1. While the GstLAL pipeline identified a low-mass marginal candidate, 151012A, in GWTC-1, the detector frame chirp mass is not covered by the bank used here. We note that five single-detector candidates meet the selection criteria for inclusion in GWTC-1 (Abbott et al. 2018b).

For 1-OGC, we define overlapping candidates as those that share coalescence times to a precision of two decimal places as differences between the pipelines and the template banks can account for small differences in the measured time of arrival. We find 15 BNS candidates in common with 1-OGC. This is not unexpected; 1-OGC has a trigger rate of $\sim$270 day^{-1} in the overlapping region of the searched parameter space. They do not assign any of the overlapping candidates a false-alarm rate of less than one per day. The variation in estimated false-alarm rates can arise from differences in the pipelines, template banks, and mass models used in the searches.

In the hopes of enabling multi-messenger, sub-threshold follow-up, we have also provided the coalescence times and sky localizations of the 103 candidates with false-alarm rates of less than 1 day^{-1}. Though localization estimates for coincident events are typically $\lesssim$1000 deg^2, the single-detector localizations trace out the approximate antenna patterns of the detector and cover most of the sky. The analysis of single-detector time yielded 15 of the 103 candidates presented in our list, and nearly half of the analyzed data was obtained during times at which only one detector was operating; this highlights the importance of continuing to analyze single-interferometer time in future GW searches.

ORCID iDs

Ryan Magee https://orcid.org/0000-0001-9769-531X
Cody Messick https://orcid.org/0000-0002-8230-3309
Leo Singer https://orcid.org/0000-0001-9898-5597

References

LIGO Scientific Collaboration, Aasi, J., Abbott, B. P., et al. 2015, CQGra, 32, 074001
Abbott, B. P., Abbott, R., Abbott, T. D., et al. 2016a, PhRvL, 116, 061102
Abbott, B. P., Abbott, R., Abbott, T. D., et al. 2016b, PhRvL, 116, 241103
Abbott, B. P., Abbott, R., Abbott, T. D., et al. 2016c, PhRvX, 6, 041015
Abbott, B. P., Abbott, R., Abbott, T. D., et al. 2016d, ApJL, 832, L21
Abbott, B. P., Abbott, R., Abbott, T. D., et al. 2016e, PhRvD, 93, 122003
Abbott, B. P., Abbott, R., Abbott, T. D., et al. 2017a, ApJL, 848, L12
Abbott, B. P., Abbott, R., Abbott, T. D., et al. 2017b, ApJ, 841, 89
Abbott, B. P., Abbott, R., Abbott, T. D., et al. 2017c, PhRvL, 119, 161101
LIGO Scientific Collaboration and Virgo Collaboration, Abbott, B. P., et al. 2018a, CQGra, 35, 065010
Abbott, B. P., Abbott, R., Abbott, T. D., et al. 2018b, CQGra, 35, 065010
Ajith, P., Babak, S., Chen, Y., et al. 2007, CQGra, 24, S689
Ajith, P., Fotopoulos, N., Privitera, S., et al. 2014, PhRvD, 89, 084041
Allen, B., Anderson, W. G., Brady, P. R., et al. 2012, PhRvD, 85, 122006
Allen, B., Blackburn, J. K., Brady, P. R., et al. 1999, PhRvL, 83, 1498
Babak, S., Biswas, R., Brady, P., et al. 2013, PhRvD, 87, 024033
Blanchet, L., Damour, T., Iyer, B. R., et al. 1995, PhRvL, 74, 3515
Buonanno, A., Iyer, B., Ochsner, E., et al. 2009, PhRvD, 80, 084043
Burns, E., Goldstein, A., Hui, C. M., et al. 2019, ApJ, 871, 90

Callister, T. A., Kanner, J. B., Massinger, T. J., et al. 2017, CQGra, 34, 155007
Cannon, K., Cariou, R., Chapman, A., et al. 2012, ApJ, 748, 136
Cannon, K., Hanna, C., & Peoples, J. 2015, arXiv:1504.04632
Cannon, K., Hanna, C., & Keppel, D. 2013, PhRvD, 88, 024025
Cannon, K. C. 2008, CQGra, 25, 105024
Dal Canton, T., & Harry, I. W. 2017, arXiv:1705.01845
Dent, T., & Veitch, J. 2014, PhRvD, 89, 062002
Dokuchaev, V. I., & Eroshenko, Y. N. 2017, arXiv:1701.02492
Essick, R. 2017, GCN, 21505, 1
Farr, W. M., Gair, J. R., Mandel, I., & Cutler, C. 2015, PhRvD, 91, 023005
Finn, L. S., & Chernoff, D. F. 1993, PhRvD, 47, 2198
Fong, H. K. Y. 2018, PhD thesis, Univ. Toronto
GstLAL, 2018, GstLAL, Software: git.ligo.org/lscsoft/gstlal
Gstreamer, 2018, Gstreamer, Software: https://gstreamer.freedesktop.org
Hanna, C., Caudill, S., Messick, C., et al. 2019, arXiv:1901.02227
Harry, I. W., Allen, B., & Sathyaprakash, B. 2009, PhRvD, 80, 104014
LIGO Scientific Collaboration 2018, LIGO Algorithm Library—LALSuite,
    Free Software (GPL), doi:10.7935/GT1W-FZ16
Messick, C., Blackburn, K., Brady, P., et al. 2017, PhRvD, 95, 042001
Mukherjee, D., Caudill, S., Magee, R., et al. 2018, arXiv:1812.05121
Nitz, A., Harry, I., Brown, D., et al. 2019a, gwastro/pycbc: Pre-O3 release v1,
    Zenodo, doi:10.5281/zenodo.2556644
Nitz, A. H., Capano, C., Nielsen, A. B., et al. 2019b, ApJ, 872, 195
Nitz, A. H., Dal Canton, T., Davis, D., & Reyes, S. 2018, PhRvD, 98, 024050
Owen, B. J. 1996, PhRvD, 53, 6749
Owen, B. J., & Sathyaprakash, B. S. 1999, PhRvD, 60, 022002
Ozel, F., Psaltis, D., Narayan, R., & Villarreal, A. S. 2012, ApJ, 757, 55
Sachdev, S., Caudill, S., Fong, H., et al. 2019, arXiv:1901.08580
Singer, L. P., & Price, L. R. 2016, PhRvD, 93, 024013
Smith, M., Fox, D., Cowen, D., et al. 2013, APh, 45, 56
Tagoshi, H., Kanda, N., Tanaka, T., et al. 2001, PhRvD, 63, 062001
Thorsett, S. E., & Chakrabarty, D. 1999, ApJ, 512, 288
Totani, T. 2013, PASJ, 65, L12
Usman, S. A., Nitz, A. H., Harry, I. W., et al. 2016, CQGra, 33, 215004
Vallisneri, M., Kanner, J., Williams, R., et al. 2015, J. Phys. Conf. Ser., 610,
    012021
Wang, J.-S., Yang, Y.-P., Wu, X.-F., et al. 2016, ApJL, 822, L7